AN ABSTRACT OF THE THESIS OF

Joseph W. Anderson for the degree of Honors Baccalaureate of Science in Chemical Engineering presented on May 29th, 2013. Title: Protection of *Nitrosomonas europaea* from Silver Nanoparticle-Induced Inhibition through a Two-Step, Magnesium-Facilitated Mechanism

Abstract Approved:

_____

Lewis Semprini

The inhibitory effects of (Ag^+) and silver nanoparticles (Ag NP) 3-5 nm in diameter (stabilized with polyvinylpyrrolidone (PVP)) and 20 nm (stabilized with citrate) on nitrification rates of the model ammonia-oxidizing bacteria (AOB) *Nitrosomonas europaea* were investigated. Experimental solutions contained HEPES buffer and ammonia (NH_3) in the presence and absence of 730 μM Mg^{2+}. Ag^+ showed the most inhibition, and Ag NP-induced inhibition decreased with increasing size. In each case, Mg^{2+} showed protection from nitrification inhibiton. Ag incorporated with the cells was measured by centrifuging experimental fluid, acid-digesting the cell pellet, and measuring via ICP-OES analysis for Ag-content of the digestion. Results indicated that less Ag incorporated with the cells in the presence of Mg^{2+}, suggesting that Mg^{2+} inhibits the sorption of Ag to *N. europaea.* UV-vis spectrophotometric analysis over 25 minutes was used to observe rapid aggregation with minimal dissolution of 20 nm citrate-stabilized Ag NP in media with 730 μM Mg^{2+}, and dissolution without aggregation of the Ag NP in media without Mg^{2+}. This suggests that Mg^{2+} prevents Ag NP-induced nitrification inhibition of *N. europaea* via a two-step mechanism: Mg^{2+} induces the aggregation of Ag NP, reducing the release of Ag^+, and prevents incorporation of Ag to cells.

Key Words: *Nitrosomonas europaea*, silver nanoparticles, nitrification inhibition

Corresponding email address: anderson.joe.w@gmail.com

Protection of *Nitrosomonas europaea* from Silver Nanoparticle-Induced Inhibition through a Two-Step, Magnesium-Facilitated Mechanism

By

Joseph W. Anderson

A PROJECT

submitted to

Oregon State University

University Honors College

in partial fulfillment of

the requirements for the

degree of

Honors Baccalaureate of Science in Chemical Engineering (Honors Scholar)

Presented May 29, 2013

Commencement June 2013

Honors Baccalaureate of Chemical Engineering project of Joseph W. Anderson presented on May 29, 2013.

APPROVED:

_____

Co-Mentor, representing Environmental Engineering

_____

Co-Mentor, representing Environmental Engineering

_____

Committee Member, representing Environmental Engineering

_____

Department Head, Chemical Engineering

_____

Dean, University Honors College

I understand that my project will become part of the permanent collection of Oregon State University, University Honors College. My signature below authorizes release of my project to any reader upon request.

_____

Joseph W. Anderson, Author

Acknowledgements

First, thank you to Dr. Lewis Semprini for being my mentor in this project, for giving me a home in your lab throughout my undergraduate career, and for your advice and assistance as I performed experiments and wrote my thesis. Your insight was invaluable with regards to the thesis and your interest in my success helped me very much in the last four years.

Thank you to Dr. Jeffrey Nason for serving on my thesis committee and helping with the editing process, and thank you to JR Giska and Margaret Schneider for your help with hours of inhibition experiments and ICP analysis.

Thank you to Hayley Moen, for your emotional and culinary support during the thesis process.

Thank you to my parents, John & Jean Anderson, for all of your support and encouragement not only during the thesis process, but also throughout my life. Without your help I would not have been able to achieve the success I have found, and it has taken a long time for me to get here. Thank you for your patience and love you give me every day.

Finally, thank you to Dr. Tyler Radniecki, who took me under his wing nearly four years ago and taught me everything I know about working in a lab. Your support has helped me grow as a researcher, as an engineer, and as a person. Oregon State University is lucky to have you back.

Funding was provided by The Pete and Rosalie Johnson Scholarship Fund, The Subsurface Biosphere Initiative, and the University Honors College Experience Scholarship.

Table of Contents

List of Figures

List of Tables

This thesis is dedicated to my parents,

who taught me to work hard

and to strive to go above and beyond in all I do.

INTRODUCTION

Ammonia-oxidizing bacteria (AOB), including *Nitrosomonas europaea*, are an integral part of the global nitrogen cycle as they oxidize ammonia (NH_3) into nitrite (NO_2^-) (Arp & Sayavedra-Soto, 2002). This function is particularly important in wastewater treatment plants (WWTPs). When this process is interrupted, unoxidized NH_3 proceeds through the treatment plant. NH_3 in surface water can cause eutrophication and result in algae blooms in downstream aquatic ecosystems. An algal population blooms until the water system becomes deficient in another limiting growth reagent, at which point the algal population begins to die. When the algae dies, it decays, which requires oxygen. This leads to low dissolved oxygen concentrations and dead zones (EPA, 1993).

AOB are very sensitive to inhibitors, due to their unique use of NH_3 as an energy source. NH_3 is not an energy-rich nutrient, which is the reason for AOB's slow rate of growth (Arp & Sayavedra-Soto, 2002). AOB's ability to oxidize NH_3 can be severely inhibited by organic hydrocarbons, heavy metals, and other antibacterials, including silver (Ag) and silver nanoparticles (Ag NP) (Radniecki, et al., 2011) (Radniecki, et al., 2008). Thus, the presence of these inhibitors may result in the release of NH_3 from WWTP into receiving bodies of water, causing eutrophication to occur.

Nanotechnology is a relatively new field that has seen great advances in the last decade. Nanotechnology encompasses any material or particle that measures between 1 and 100 nm in at least one dimension (ASTM, 2012). Properties of nanomaterials can differ from the properties of bulk materials or dissolved materials in solution that have the same chemical composition (Auffan, et al., 2009). Nanomaterials have been developed from metals (e.g. Ag, Au), metal oxides, (e.g. TiO_2, Fe_2O_3, ZnO, SiO_2) and carbon-based structures (e.g. carbon nanotubes and fullerenes) (Mueller & Nowack, 2008) (Wiesner, et al., 2009). The rapid advances in

nanotechnology, however, has left a gap in the knowledge on the environmental impacts of nanomaterials (Kulinowski, 2008) (Roco, 2005).

Ag has antimicrobial properties that have been utilized for many years in numerous applications. Recent advances in the field of nanotechnology offers new ways to design and manufacture Ag applications, through the use of Ag NPs that will release Ag^+ into solution over time. This effect is desirable in products like garments or textiles to control odors and cleaning appliances to sanitize dishes or clothing and the slow-release technique has the potential to increase the useful life of the product.

Ag NPs have been identified as the most widely used type of nanoparticle in consumer goods (being found in over 50% of nanoparticle-containing products) (The Project on Emerging Nanotechnologies, 2009). Silver in a nanoparticle form retains the anti-microbial characteristics of Ag^+ and have been used in medical equipment and household goods including odor-reducing garments, textiles, and sanitizing equipment (dishwashers, washing machines, etc.) (Benn & Westerhoff, 2008).

Research has shown that Ag NPs in these applications are released either inadvertently (through the washing of the textiles) or intentionally (as used in sanitizing appliances) into commercial and residential wastewater systems. Other research has shown that Ag^+ and Ag NP can bioaccumulate in WWTP biosolids (EPA, 2009), (Benn & Westerhoff, 2008) and therefore have the potential to interfere with critical WWTP functions, such as the nitrification process performed by AOB (Radniecki, et al., 2011) (Giao & Limpiyakorn, 2012).

N. europaea, a model AOB, has been used in numerous studies to investigate phenomena affecting AOB (Arp & Sayavedra-Soto, 2002). Literature suggests that the relative toxicity of Ag NP depended on their size, surface chemistries, and the aquatic environments in which they were suspended (Radniecki, et al., 2011) (Arnaout & Gunsch, 2012) (Yuan, et al., 2013). All of these

factors influence the rate of release of Ag^+ into the aqueous phase. Work performed by Radniecki et. al. (2011) suggests that the decrease of nitrification activity observed in *N. europaea* in the presence of Ag NP is due to the amount of released Ag^+ in solution. Choi et. al., (2008) however identifies additional toxic effects of the nanoparticles on AOB. The lack of a consensus on the impact of Ag NP on AOB reflects the same phenomena in the greater field of nanotechnology and proves the need for further research and understanding on the topic.

Initial data suggests that the presence of Mg^{2+} influences Ag^+- and Ag NP-induced nitrification inhibition of *N. europaea*. This study further investigates the effects of Mg^{2+} on Ag^+ and Ag NP toxicity and experiments were designed to help identify potential mechanisms of observed Mg^{2+} protective effects. This work will be the first to provide a detailed mechanism to show how Mg^{2+} prevents Ag NP and Ag^+ inhibition of nitrification activity.

Experiments presented in this work investigated nitrification rates of *N. europaea* in the presence of Ag^+ and Ag NP, with and without Mg^{2+}. *N. europaea* cells from these experiments were isolated and the amount of Ag incorporated with cells was quantified via ICP analysis. The concentration of Ag NPs remaining in solution was also investigated, via UV-vis spectroscopy, to observe the absorbance-related phenomena that occurred in the presence of various media components. Results obtained from these experiments were used to develop a proposed two-step Mg^{2+}-facilitated mechanism for the protection of *N. europaea* from Ag NP-induced inhibition.

MATERIALS & METHODS

N. europaea culturing methods

N. europaea ATCC 19718 cells were grown in the dark at 30 °C and shook at 150 RPM for a period of 3 d in 2 L of media, containing KH_2PO_4 (at pH 7.8), $(NH_4)_2SO_4$, $CaCO_3$, $MgSO_4$, $CaCl_2$, $FeSO_4$, EDTA (used to suspend the stock solution of $FeSO_4$), and $CuCl_2$ (Radniecki, et al., 2011). Cells were harvested via centrifugation at 9000 RPM, for 1 h during the mid-exponential growth phase, at an OD_{600} of approximately 0.070. The cells were resuspended in 30 mL of 30 mM HEPES buffer (pH 7.8), centrifuged once again at 9000 RPM for 30 min and resuspended in 30 mL of 30 mM HEPES buffer (pH 7.8). Cells were stored in the centrifuge tube at 10 °C until used for an experiment.

General inhibition experiment procedure

The inhibitory effects of different forms of Ag in the presence and absence of Mg^{2+} were investigated according to a general protocol outlined as follows. Specifics of each experiment are described in the following sections.

Ag NP were obtained from nanoComposix (Biopure, citrate-stabilized 20 nm particles, suspended in a 2 mM sodium citrate buffer, and Biopure, PVP-stabilized 3-5 nm particles, suspended in water).

155 mL batch bioreactors containing nanopure deionized water were dosed with Ag (either as $AgNO_3$ or Ag NPs), in order to disperse the Ag in the solution. The bioreactor bottles were then shaken in the dark at 250 RPM at 30 °C for 1 h. Control reactors containing no Ag were also shaken for 1 h under the same conditions. A 15x concentrated solution of HEPES and $(NH_4)_2SO_4$ was then added to final concentrations of 30 mM and 2.5 mM, respectively. Previous research discusses how introduction of Ag NP into a solution of high ionic strength induces immediate,

rapid aggregation (Huynh & Chen, 2011), and that introduction of Ag NP before media constituents (buffer and NH_3) will not cause immediate aggregation (Radniecki, et al., 2011).

In treatment sets that received Mg^{2+}, a concentrated Mg^{2+} solution was also added at this time. The reactors were shaken at the conditions described above for another 30 min and inoculated with *N. europaea* to a concentration of 5 mg protein/L (approximately an OD_{600} of 0.060). The batch bottles were shaken for an additional 180 min, with samples taken every 45 min for NO_2^- analysis, starting immediately after the addition of the cells.

NO_2^- concentrations were measured via a colorometric assay by mixing 10 µL of the experimental solution with 890 µL of 1% w/v sulphanilamide in 1 M HCl and 100 µL of 0.2% w/v n-1 napthyl-ethyldiamine. The sample was fully mixed and after 10 min the absorbance was measured at 540 nm using a spectrophotometer. Absorbance was compared to a linear standard curve to calculate NO_2^- concentration in the sample (Appendix - Figure 17).

Relative nitrification activity was measured by relating the NO_2^- produced by the cells over a period of time in the treatment bottles to that in the control bottles, both normalized to the respective cell densities in each reactor. For the purposes of this paper, percent nitrification activity was calculated via Equation 1 and will be used for most of the analyses presented herein.

Equation 1

$$Percent\ Nitrification\ Activity = \left(\frac{\frac{[NO^{2-}]}{[protein]} \left(\frac{mmol}{mg}\right)\Big|_{t=180,treatment}}{\frac{[NO^{2-}]}{[protein]} \left(\frac{mmol}{mg}\right)\Big|_{t=180,control}} \right) * 100\%$$

Protein concentrations were calculated by measuring the absorbance of a 1 mL sample from each reactor at 600 nm and comparing it to a previously developed linear standard curve relating absorbance to protein concentration (Radniecki, et al., 2011).

Upon completion of select 3h inhibition experiments, 30-45 mL of test solution from each reactor was centrifuged for 20 min at 9000 RPM to pellet the cells and any adsorbed Ag. A 6 mL sample of the supernatant was saved and mixed with 100 µL of 36 N H_2SO_4 to a final concentration of 0.59 N H_2SO_4 and incubated at room temperature for 18 h.

The rest of the supernatant was decanted and the cell pellet from the 30-45 mL of media was resuspended in 500 of µL nanopure deionized water and digested overnight at 60 °C in a solution of 2.5 mL of 15.7 N nitric acid and 500 µL of 85% phosphoric acid (to final concentrations of 11.2 N nitric acid and 12% phosphoric acid). Pellet digestions were then diluted 2x in deionized water before being measured using a Teledyne Leeman Prodigy ICP-OES (Hudson, NH, USA).

Ag species in the presence of Mg^{2+}

An experiment was designed to investigate the effect of Ag^{+}, 3-5 nm polyvinylpyrrolidone (PVP)-stabilized Ag PN, and 20 nm citrate-stabilized Ag NP on *N. europaea* nitrification rates in the presence and absence of Mg^{2+}. This experiment was performed to observe whether protective effects of Mg^{2+} on Ag-induced inhibition resembled the protective effects observed in the case of Zn^{2+}- and Cd^{2+}-induced inhibition (Radniecki, et al., 2008). Sets of bioreactors were prepared as described above with 46.7 mL deionized water to contain final concentrations of 0.1 ppm Ag^{+}, 0.14 ppm 3-5 nm PVP-stabilized Ag NP, or 0.75 ppm 20 nm citrate-stabilized Ag NP. 3.3 mL of the 15x concentrated HEPES and $(NH_4)_2SO_4$ solution added to make a final volume of 50 mL and concentrations of 30 mM HEPES and 2.5 mM $(NH_4)_2SO_4$.

Mg^{2+} was added to additional bottle sets of each Ag concentration (and controls with no Ag) to final concentrations of 200 and 730 µM Mg^{2+}. All conditions were conducted in triplicate.

Ag^{+} with Mg^{2+} dose response with Ag sorption analysis

An experiment was designed to observe protective effects of a range of Mg^{2+} concentrations on a constant concentration of Ag^{+}, and to observe Ag adsorption to cells in each case. Sets of bioreactors were prepared as described above with 46.7 mL deionized water to contain final concentrations of 0.5 ppm Ag^{+}. 3.3 mL of the 15x concentrated HEPES and $(NH_4)_2SO_4$ solution added to make a final volume of 50 mL and concentrations of 30 mM HEPES and 2.5 mM $(NH_4)_2SO_4$. Another set of control bottles containing no Ag in any form was also prepared. Mg^{2+} was added as outlined above to triplicate bottle sets containing both Ag^{+} and no Ag^{+} to final concentrations of 50, 200, and 730 µM Mg^{2+}. Upon completion of the 180 min inhibition investigation, cells in 45 mL of experimental solution from each reactor were harvested for ICP analysis as described above.

Ag^{+} dose response with Mg^{2+} with Ag sorption analysis

An experiment was designed to observe protective effects of Mg^{2+} on a range of concentrations of Ag^{+}, and to observe Ag adsorption to cells in each case. Sets of bioreactors were prepared as described above with 46.7 mL deionized water to contain final concentrations of 0.1, 0.5, and 1.0 ppm Ag^{+}. 3.3 mL of the 15x concentrated HEPES and $(NH_4)_2SO_4$ solution added to make a final volume of 50 mL and concentrations of 30 mM HEPES and 2.5 mM $(NH_4)_2SO_4$. Another set of control bottles containing no Ag in any form was also prepared. Mg^{2+} was added as outlined above to triplicate bottle sets containing each concentration of Ag^{+} and the control set to a final concentration of 730 µM Mg^{2+}. Another set ran in parallel which contained no Mg^{2+}. Upon completion of the 180 min inhibition investigation, cells in 45 mL of experimental solution from each reactor were harvested for ICP analysis as described above.

Ag NP dose response with Mg^{2+} with Ag sorption analysis

An experiment was designed to observe protective effects of Mg^{2+} on a range of concentrations of Ag NP, and to observe Ag adsorption to cells in each case. Sets of bioreactors were prepared as

described above with 32.7 mL deionized water to contain final concentrations of 0.4, 2.0, and 4.0 ppm 20 nm citrate-stabilized Ag NP. 2.3 mL of the 15x concentrated HEPES and $(NH_4)_2SO_4$ solution was added to make a final volume of 35 mL and concentrations of 30 mM HEPES and 2.5 mM $(NH_4)_2SO_4$. Another set of control bottles containing no Ag NPs was also prepared. Mg^{2+} was added as outlined above to triplicate bottle sets containing each concentration of Ag NPs and the control set to a final concentration of 730 µM Mg^{2+}. Another set ran in parallel which contained no Mg^{2+}. Upon completion of the 180 min inhibition investigation, cells in 30 mL of experimental solution from each reactor were harvested for ICP analysis as described above.

Table 1. Summary of experiments.

Experiment Number	Ag Form	Ag (ppm)	Mg^{2+} (µM)	ICP Analysis
1	Ag^+	0.10	200, 730	No
	Ag NP (3-5 nm, PVP stabilized)	0.14		
	Ag NP (20 nm, citrate stabilized)	0.75		
2	Ag^+	0.5	50, 200, 730	Yes
3	Ag^+	0.1, 0.5, 1.0	730	Yes
4	Ag NP (20 nm, citrate stabilized	0.4, 2.0, 4.0	730	Yes

Spectrophotometric analysis of structural change phenomena

Oscillation of electrons on the surface of Ag NP induced by an electromagnetic field (surface plasmon resonance) absorbs at approximately 400 nm (Ostermeyer, 2012) (Delay, et al., 2011) (Seney, et al., 2009) (Zook, et al., 2011). UV-vis analysis was used to observe 1.0 ppm 20 nm citrate-stabilized Ag NP in deionized water, and in the presence of 30 mM HEPES (pH 7.8), 2.5 mM $(NH_4)_2SO_4$, with 0 and 730 µM Mg^{2+}. The batch reactors were prepared as described in the Ag NP dose response section, in the absence of *N. europaea*. A 1.0 mL sample of liquid was taken immediately after introducing Mg^{2+} and the HEPES/$(NH_4)_2SO_4$ solution and every 5 minutes after for 25 minutes. The adsorbance of the samples were measured with a UV-vis spectrophotometer between 300 and 600 nm.

RESULTS & DISCUSSION

Toxicity of ionic silver and silver nanoparticles in the absence or presence of Mg^{2+}

Higher concentrations of Ag were required to produce the same inhibitory effects with increasing nanoparticle size (Figure 1), as has been observed before in literature (Radniecki, et al., 2011) (Yuan, et al., 2013). Ag^{+} required a concentration of 0.1 ppm to inhibit the cells to 17.3% ± 5.7% activity, while concentrations of 0.14 ppm 3-5 nm PVP-stabilized Ag NP and 0.75 ppm 20 nm citrate-stabilized Ag NP were required to achieve similar effects (16.0% ± 1.3% and 20.1% ± 4.1%, respectively). The presence of 200 µM Mg^{2+} increased nitrification activity in the case of each Ag form to approximately 75% and the presence of 730 µM Mg^{2+} produced nearly complete protection in the case of Ag^{+} and 20 nm citrate-stabilized Ag NP (98.8% ± 13% and 97.7% ± 4.6% respectively. With 730 µM Mg^{2+}, 0.14 ppm 3-5 nm PVP-stabilized Ag NP still inhibited nitrification activity to 83.8% ± 7.1%. This protective effect of Mg^{2+} has also been observed in instances in which Zn^{2+} and Cd^{2+} were investigated as inhibitors to nitrification activity (Radniecki, et al., 2008).

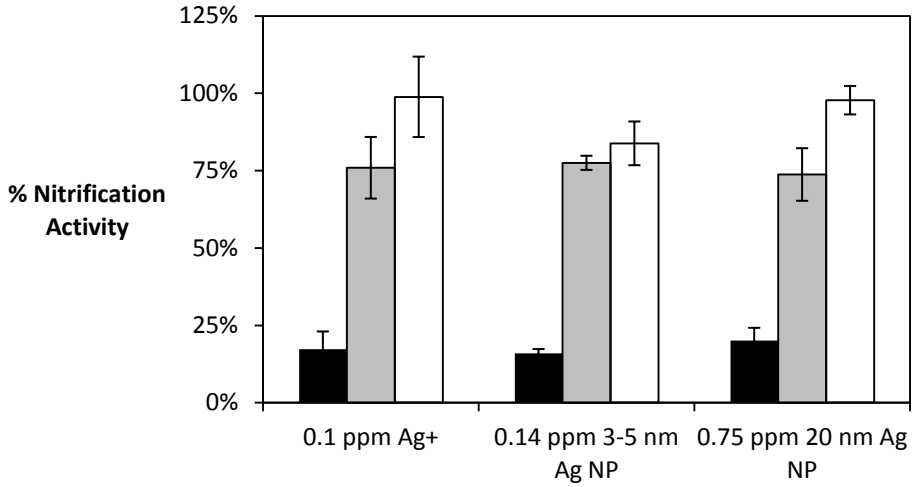

Figure 1. Percent nitrification activity of *N. europaea* in the presence of different silver forms and 0(■), 200 (▨), and 730 µM (□) $MgSO_4$. Error bars represent 95% confidence intervals from triplicate experiments.

Mechanism 1:

Mg^{2+} in solution protects *N. europaea* from toxic effects of Ag^{+}

N. europaea cells exposed to 0.5 ppm Ag^{+} showed increasing activity with increasing Mg^{2+} concentration (Figure 2). At 0.5 ppm Ag^{+} and an absence of Mg^{2+}, *N. europaea* were inhibited to 17% activity, but increasing Mg^{2+} concentrations saw activity rise to 67% in the presence of 730 µM $MgSO_4$ (Figures 2 and 3).

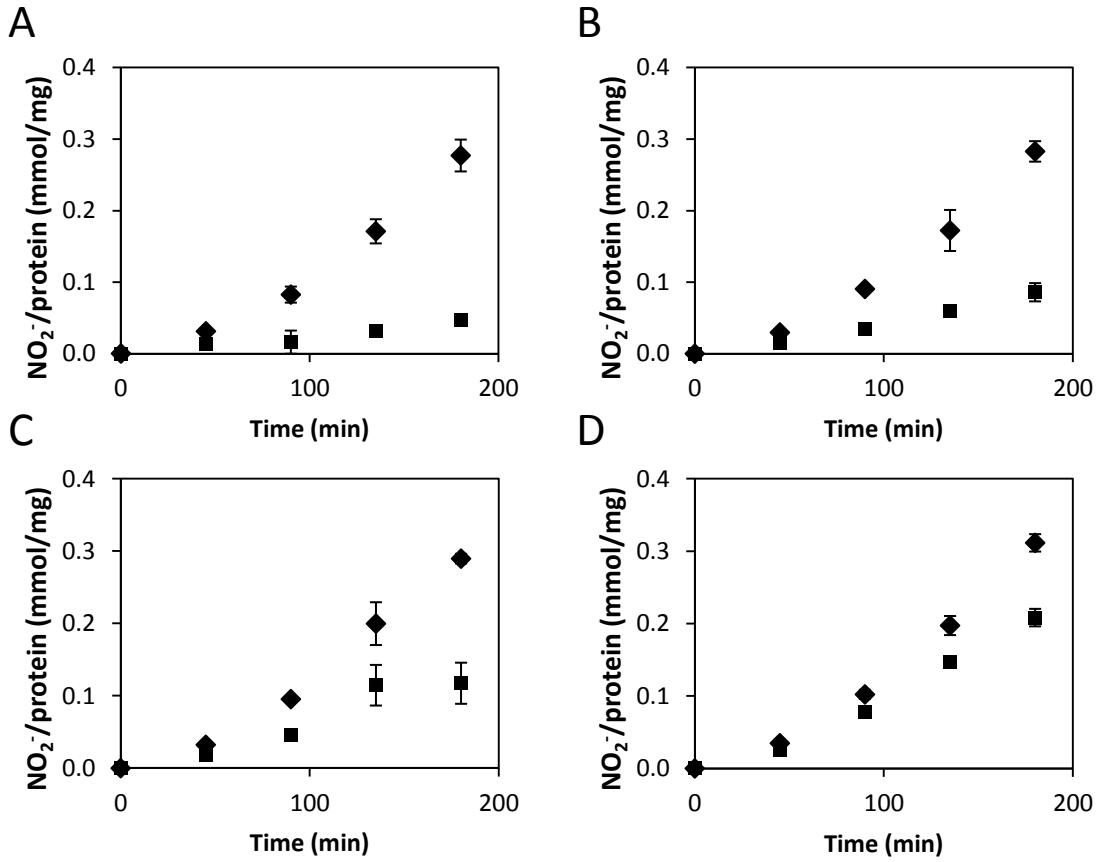

Figure 2. NO_2^- concentration in reactors normalized to cell density over time at 0 (◆) or 0.5 (■) ppm Ag^{+} in 0 (A), 50 (B), 200 (C), and 730 (D) µM Mg^{2+}. Error bars represent 95% confidence intervals from triplicate experiments.

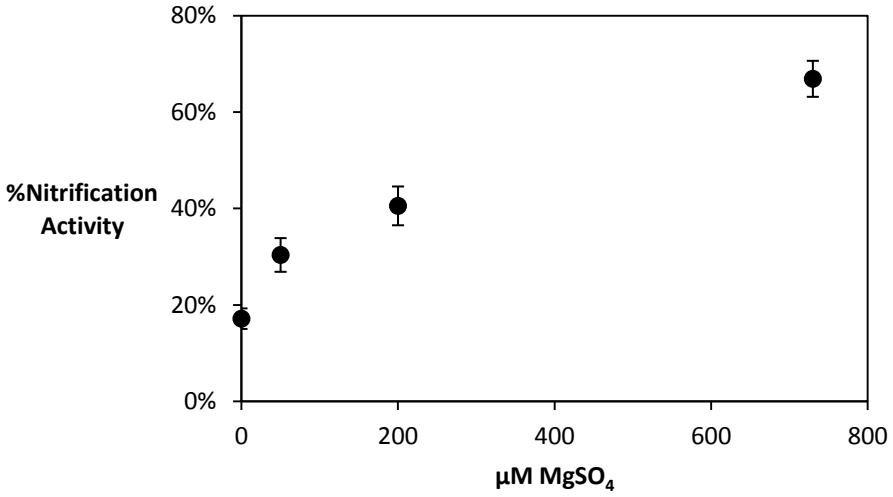

Figure 3. Percent nitrification activity of *N. europaea* in the presence of varying concentrations of Mg^{2+} and 0.5 ppm Ag^{+} vs. Ag-absent controls. Error bars represent 95% confidence intervals from triplicate experiments.

ICP-OES analysis of the pelleted and digested cells that produced Figures 2 and 3 yielded sorbed Ag per cell mass concentrations depicted in Figure 4. As Mg^{2+} concentrations increased, the Ag that was sorbed to the cells decreased from 0.009 ± 0.0012 mg Ag/mg protein (with no Mg^{2+} present) to 0.0015 ± 0.0016 mg Ag/mg protein (with 730 µM Mg^{2+} present). The large amount of variation in the samples made it difficult to identify an exact trend, but comparing the two extreme values showed that only about 17% of the Ag that was sorbed to the cells in the absence of Mg^{2+} was observed on the cells in the presence of 730 µM Mg^{2+}.

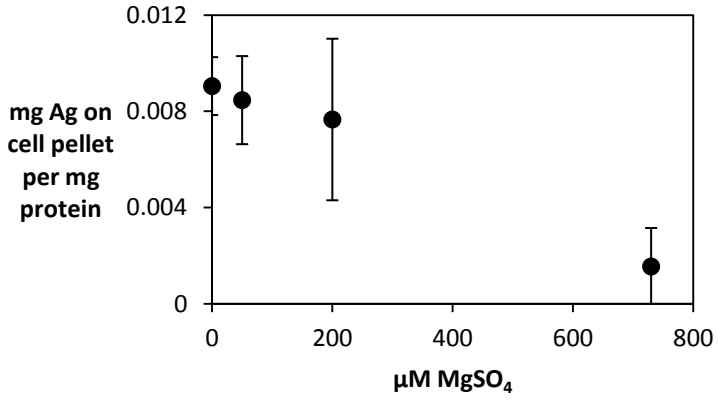

Figure 4. mg Ag^{+} per mg protein vs. Mg^{2+} concentration with 0.5 ppm Ag^{+}. Error bars represent 95% confidence intervals from triplicate experiments.

Two additional experiments were designed to investigate the same phenomena of Mg^{2+} preventing Ag incorporation with the cells, but in the presence of constant Mg^{2+} concentration (730 µM) and over a range of concentrations of both Ag^{+} and Ag NP. Increasing Ag^{+} concentrations with constant HEPES, NH_3, and cell concentrations produced decreasing nitrification rates. Plots of measured NO_2^- production rates of *N. europaea* exposed to Ag shows the trend of decreasing activity with increasing Ag^{+} concentrations in the absence (Figure 5A) and presence (Figure 5B)of 730 µM Mg^{2+}.

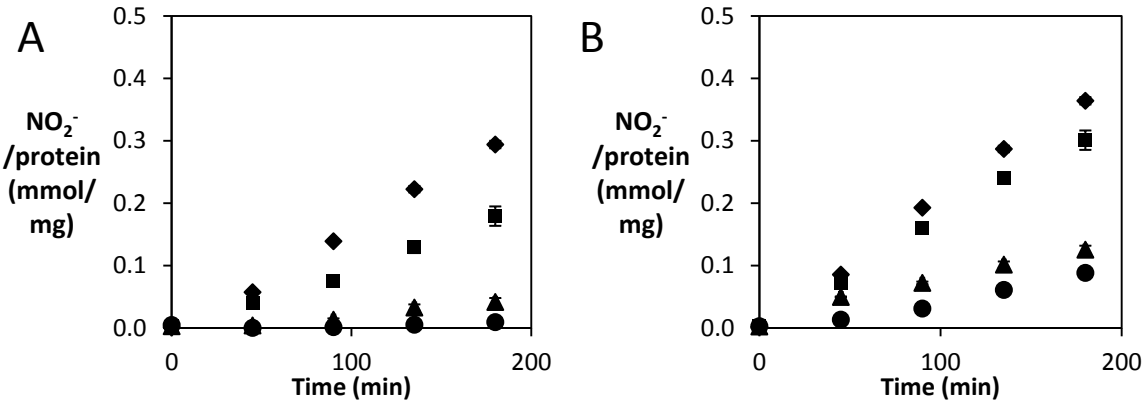

Figure 5. NO_2^- concentration in reactors normalized to cell density over time at 0 (◆), 0.1 (■), 0.5 (▲), and 1.0 (●) ppm Ag^{+} in the absence (A) and presence (B) of 730 µM Mg^{2+}. Error bars represent 95% confidence intervals from triplicate experiments.

Values for percent nitrification activity are listed in Table 2 and displayed in Figure 6. Presence of increasing Ag^{+} inhibited nitrification rates, to as low as 3.2% ± 0.5% at 1.0 ppm. The presence of 730 µM Mg^{2+} resulted in an increase in nitrification activity during exposure to Ag^{+}, to 24.2% ± 1.7%. Retained activity from Mg^{2+} equaled approximately 20% activity in each Ag^{+} concentration investigated.

Table 2. Percent nitrification activity of *N. europaea* cells exposed to different concentrations of Ag^{+} in the presence and absence of 730 µM Mg^{2+}

	0.1 ppm Ag^{+}	0.5 ppm Ag^{+}	1.0 ppm Ag^{+}
0 µM Mg^{2+}	61.0% ± 4.6%	14.2% ± 1.7%	3.2% ± 0.5%
730 µM Mg^{2+}	82.7% ± 6.0%	34.4% ± 2.2%	24.2% ± 1.7%

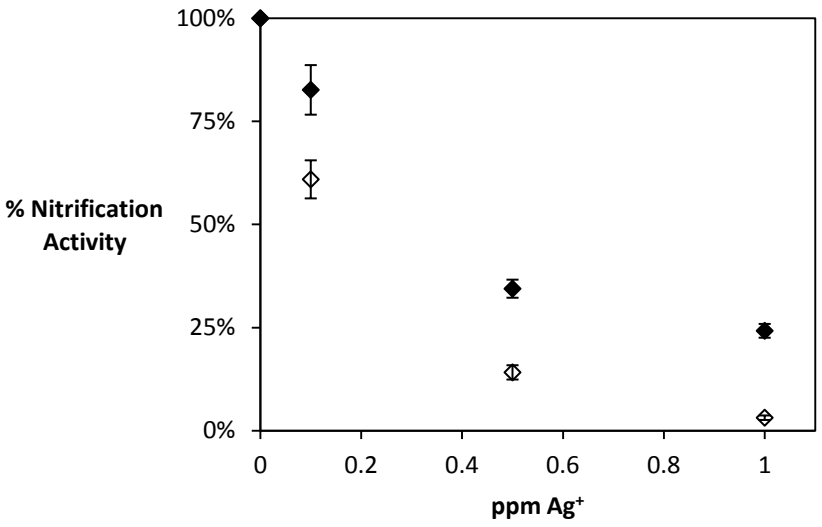

Figure 6. Percent nitrification activity of *N. europaea* in the presence of a range of Ag^{+} in the presence (◆) and absence (◇) of 730 µM Mg^{2+} vs. Ag-absent controls. Error bars represent 95% confidence intervals from triplicate experiments.

ICP analysis of the cell pellets isolated from the experiments which produced Figures 5 & 6 showed that the presence of Mg^{2+} led to decreased Ag observed in the cell pellets (Figure 8). With constant Mg^{2+} concentration (730 µM Mg^{2+}), approximately 75% less Ag was observed in the cell pellet at different Ag^{+} concentrations.

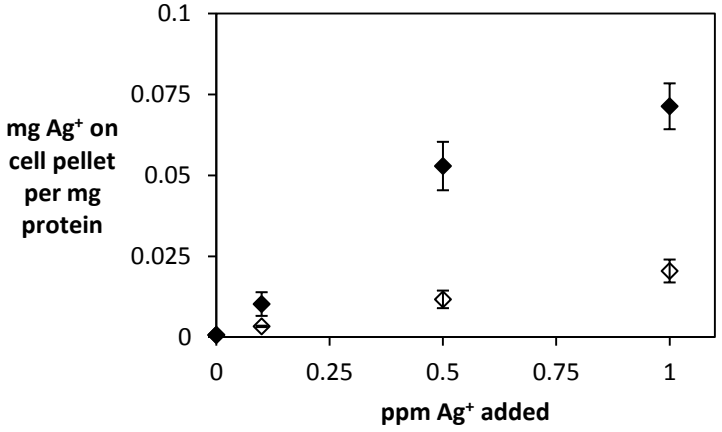

Figure 7. mg Ag per mg protein vs. Ag^{+} concentration in the presence (◇) and absence (◆) of 730 µM Mg^{2+}. Error bars represent 95% confidence intervals from triplicate experiments.

Likewise, increasing Ag NP concentrations produced decreasing nitrification activity over the range of Ag NP concentrations investigated. A plot of measured NO_2^- production rates of *N. europaea* exposed to 20 nm citrate-stabilized Ag NP shows the trend of decreasing activity with increasing Ag NP concentration (Figure 8A). NO_2^- production rates of *N. europaea* in the same concentrations of Ag NP with added 730 µM Mg^{2+} is presented in Figure 8B.

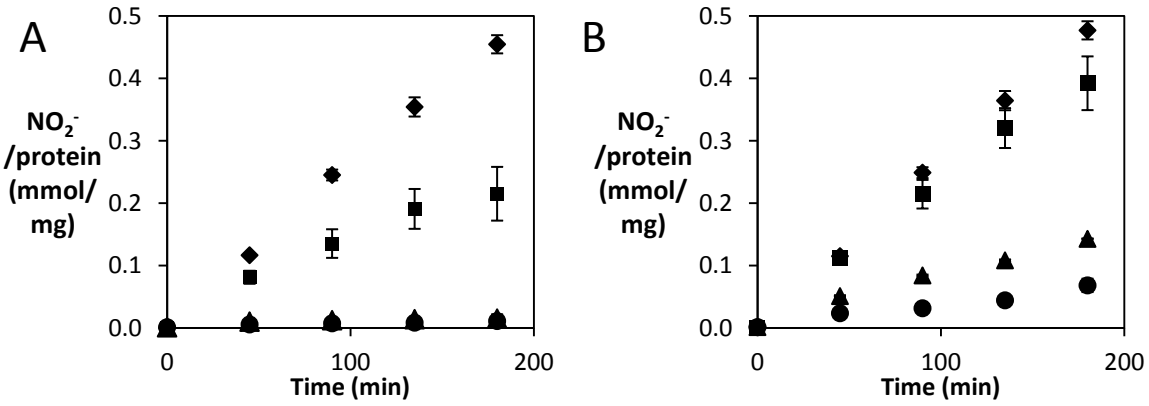

Figure 8. NO_2^- concentration in reactors normalized to cell density over time at 0 (◆), 0.4 (■), 2.0 (▲), and 4.0 (●) ppm 20 nm citrate-stabilized Ag NP in the absence (A) and presence (B) of 730 µM Mg^{2+}. Error bars represent 95% confidence intervals from triplicate experiments.

Values for percent nitrification activity are listed in Table 2 and displayed in Figure 9. Increasing 20 nm citrate-stabilized Ag NP concentrations to 4 ppm inhibited nitritification rates to as low as 2.5% ± 0.1%. The presence of 730 µM Mg^{2+} resulted in an increase in nitrification activity during exposure to Ag NP, up to 14.3% ± 1.7% with 4.0 ppm Ag NP. This data series did not show constant protection effects, with retained activity measurements ranging between approximately 35% (in 0.4 ppm Ag NP) and approximately 10% (at 4.0 ppm Ag NP).

Table 3. Percent nitrification activity of *N. europaea* cells exposed different concentrations of 20 nm citrate-stabilized Ag NP in the presence and absence of 730 µM Mg^{2+}

	0.4 ppm Ag NP	2.0 ppm Ag NP	4.0 ppm Ag NP
0 µM Mg^{2+}	47.3% ± 7.8%	3.3% ± 0.2%	2.5% ± 0.1%
730 µM Mg^{2+}	82.2% ± 2.6%	30.0% ± 5.3%	14.3% ± 1.7%

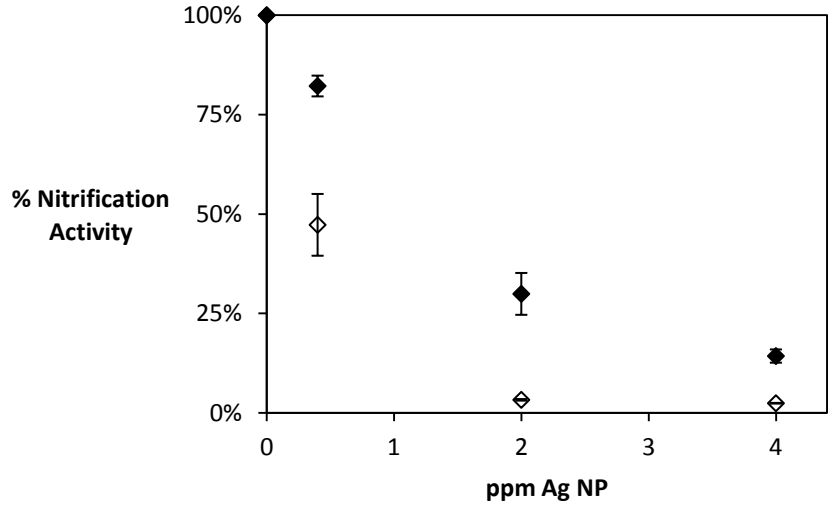

Figure 9. Percent nitrification activity of *N. europaea* in the presence of a range of 20 nm citrate- stabilized Ag NP in the presence (◆) and absence (◇) of 730 µM Mg^{2+} vs. Ag-absent controls. Error bars represent 95% confidence intervals from triplicate experiments.

ICP analysis of the cell pellets isolated from the experiments which produced Figures 8 & 9 showed that the presence of Mg^{2+} led to decreased Ag observed in the cell pellets (Figure 10). With constant Mg^{2+} concentration (730 µM Mg^{2+}), approximately 80% less Ag was observed in the cell pellet than without Mg^{2+}.

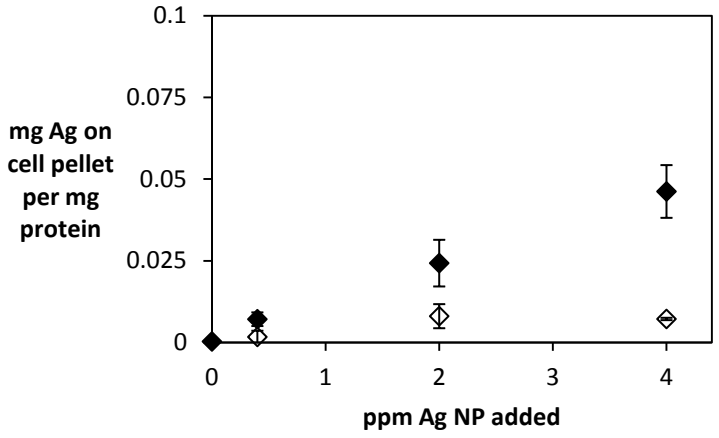

Figure 10. mg Ag per mg protein vs. Ag NP concentration in the presence (◇) and absence (◆) of 730 µM Mg^{2+}. Error bars represent 95% confidence intervals from triplicate experiments.

Experiments described in this section were designed to produce approximately comparable results for tabulated nitrification activity between Ag^{+} and Ag NP exposures. Nitrification activity results

yielded approximately similar responses, with Ag NP proving slightly more inhibitory than anticipated (Figure 11). Associated Ag (Figure 7 and 10) in the presence of Mg^{2+} relative to that retained in the absence of Mg^{2+} was approximately the same for Ag^{+} (approximately 25%) and Ag NP (approximately 20%) (Figure 12).

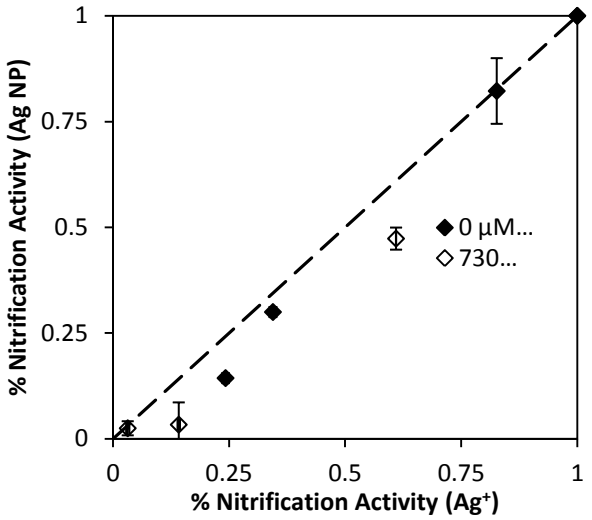

Figure 11. Percent nitrification activity of *N. europaea* in the presence of Ag NP vs. percent nitrification activity of *N. europaea* in the presence of Ag^{+} from experiments designed to produce the same inhibition in the absence (◆) and presence (◇) of 730 µM Mg^{2+}. The dashed line represents the expected trend of the data. Error bars represent 95% confidence intervals from triplicate experiments.

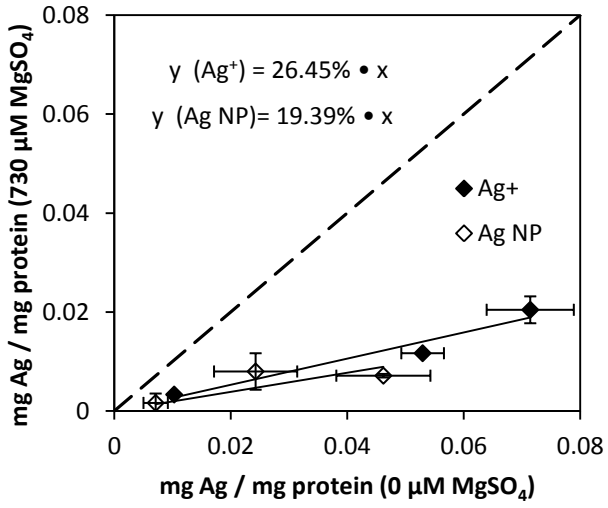

Figure 12. mg Ag per mg protein associated with the cell pellet in the presence of 730 µM Mg^{2+} vs. the same in the absence of Mg^{2+} with Ag^{+} (◆) and Ag NP (◇). The dashed line represents the trend at which point the two values will be equal.

Mechanism 2:

Mg^{2+} causes Ag NP aggregation in solution

The absorbance spectra of Ag NPs in different media were observed via UV-vis spectroscopyover time to observe structural changes in the particles as indicated by characteristic shifts in the absorbance spectra, as described in literature (Ostermeyer, 2012) (Delay, et al., 2011) (Seney, et al., 2009). Results obtained from UV-vis analysis of Ag NP aggregation and dissolution of a 1.0 ppm 20 nm citrate-stabilized Ag NP solution in different media are presented below.

A solution of only 20-nm citrate-stabilized Ag NP in deionized water is presented in Figure 13A. No change in the peak at 400 nm over the 25 minutes indicates that there is no change in the concentration and structure of the Ag NPs in solution and that the Ag NP are undergoing no aggregation or dissolution. The UV-vis results when 30 mM HEPES (pH 7.8) and 2.5 mM $(NH_4)_2SO_4$ were added are depicted in Figure 13B. This shows a gradual decrease in the peak intensity at 400 nm over 25 minutes. This is indicative of dissolution of the Ag NP into Ag^+ (Ostermeyer, 2012).

UV-vis results from 1.0 ppm 20-nm citrate-stabilized Ag NP in 30 mM HEPES (pH 7.8), 2.5 mM $(NH_4)_2SO_4$ with 730 µM Mg^{2+} are depicted in Figure 13C. A rapid drop in the peak intensity around 400 nm is indicative of a drop in the concentration of Ag NP and the gradually growing and widening band between 450 and 600 nm indicates the generation of larger Ag species. Literature suggests that the combination of these two phenomena means that the Ag NP are aggregating (Zook, et al., 2011) (Ostermeyer, 2012) (Delay, et al., 2011). This suggests that Mg^{2+} induces aggregation of the particles, decreasing their surface area to volume ratio, which inhibits the release of Ag into solution as hypothesized by Radniecki et. al. (2011).

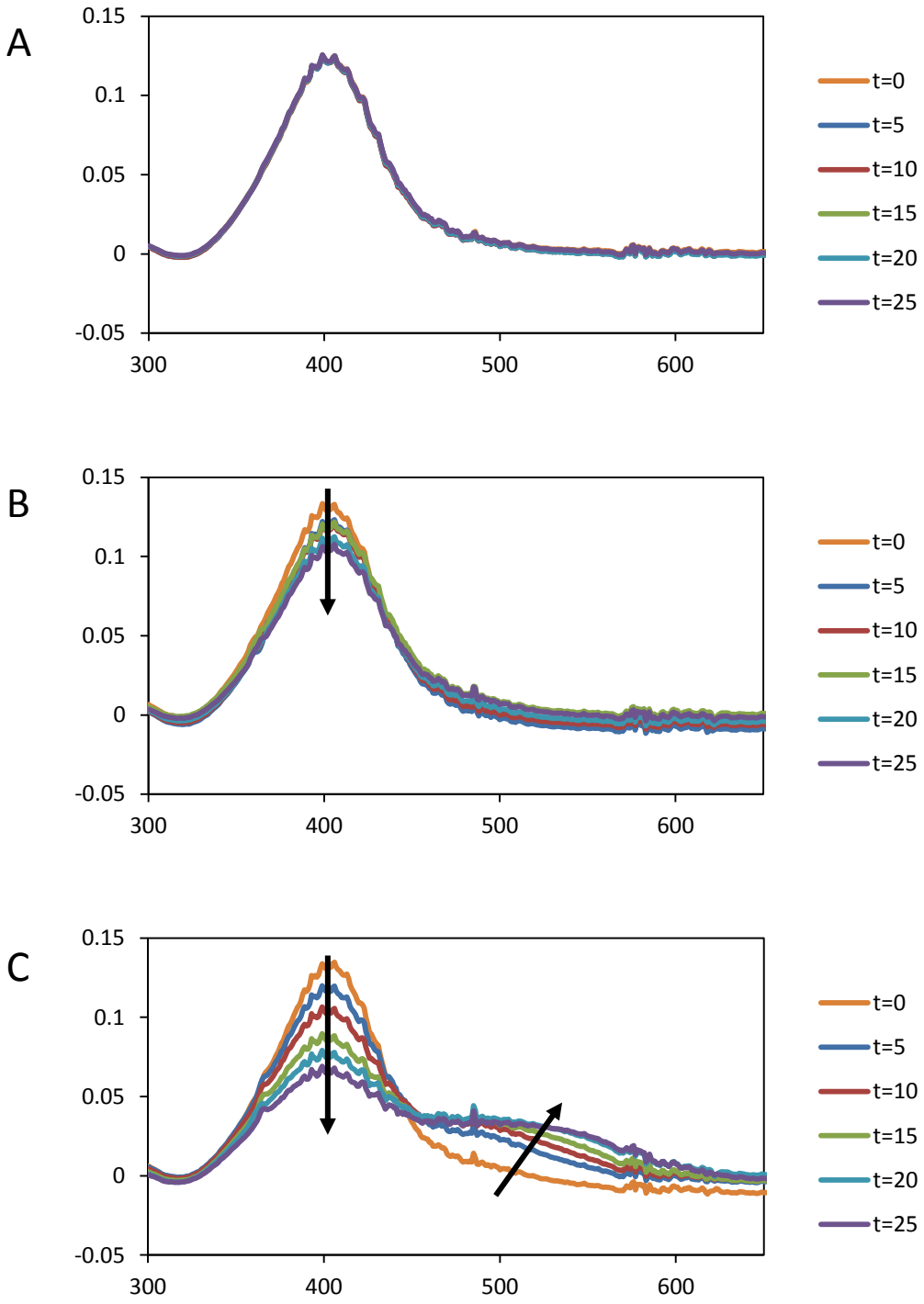

Figure 13. UV-vis spectra of 1.0 ppm Ag NP from 0 to 25 minutes with no other media constituents (A), with 30 mM HEPES (pH 7.8), and 2.5 mM $(NH_4)_2SO_4$ (B), and with730 µM Mg^{2+}, 30 mM HEPES buffer (pH 7.8), and 2.5 mM $(NH_4)_2SO_4$ (C). Arrows on plot show change in features over time.

FUTURE RESEARCH

Nitrification activity on a mg Ag per mg protein basis

Comparing percent nitrification activity from Figure 6 and Figure 9 to the mg Ag per mg protein from Figure 7 and Figure 10 yields Figure 14, which suggests some interesting trends which should be investigated in future research. Radniecki et. al. (2011) found that nitrification inhibition rates depended on the amount of Ag associated with the cells at the end of a similar 3 h experiment was the same whether the cells were exposed to Ag^{+} or Ag NP, even though the concentrations of Ag NP exposed to the cells were 5 times higher on a ppm basis. This led them to suggest that the soluble Ag dissolved from the Ag NP was responsible for Ag NP-induced inhibition.

Inspection of the data suggests a strong correlation between activity and Ag incorporated with the cells. At low associated silver (<0.02 mg Ag per mg protein) the trends of both the Ag^{+} data and the Ag NP data are statistically indiscernible, which agrees with data published by Radniecki et. al. (2011). With higher associated silver (>0.02 mg Ag per mg protein), however, activity of *N. europaea* exposed to Ag NP rapidly drops off, but when exposed to Ag^{+}, drops off more gradually. This could be due to initial nitrification rates before adsorption of Ag to the cells could occur, but inspection of Figure 5 suggests that that is not the case. More data should be taken with both Mg^{2+} present and absent to further inspect this discrepancy.

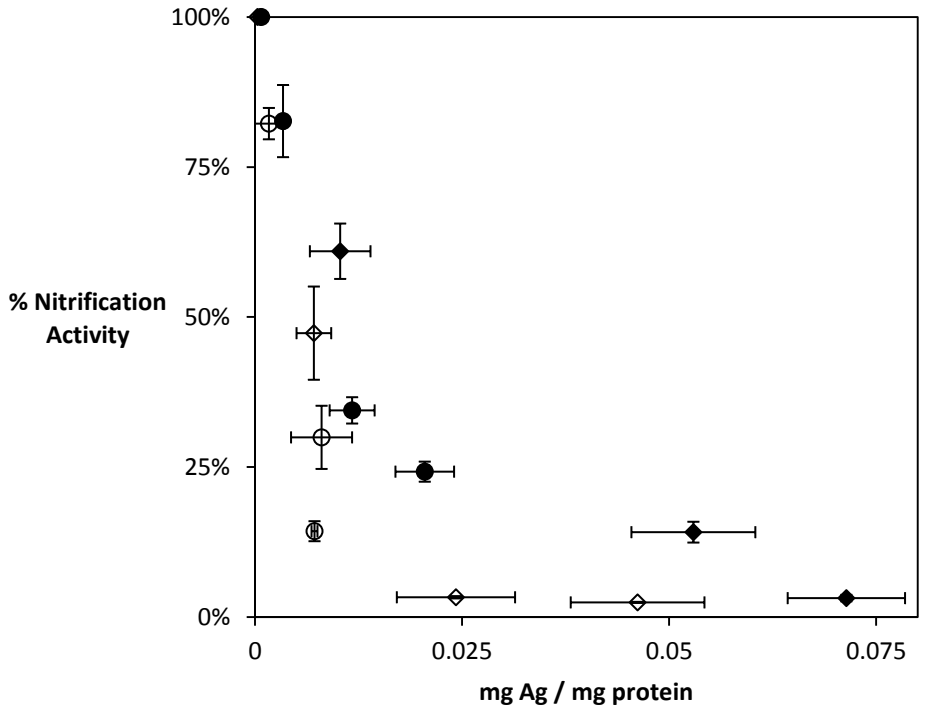

Figure 14. Percent activity of *N. europaea* vs. mg Ag per mg protein with Ag^{+} in the presence of 0 µM (◆) or 730 µM (●) Mg^{2+} and Ag NP in the presence of 0 µM (◇) or 730 µM (○) Mg^{2+}. Error bars represent 95% confidence intervals from triplicate experiments.

Other researchers have suggested that Ag NPs produce inhibitory effects by puncturing holes in the membrane of *N. europaea* (Choi & Hu, 2008) (Arnaout & Gunsch, 2012) (Yuan, et al., 2013), which could account for the difference in observed responses. Further work should be done to investigate if this phenomena occurred in the experiments performed in this study, which could be done by SEM analysis. Additionally, adsorption kinetics could be investigated by performing experiments outlined in this text, but on shorter time scales.

Observation of membrane destabilization was attempted by measuring K^{+} concentrations of the cell pellets and the experiment supernatant. A decrease in K^{+} concentration in the cell pellet (and corresponding increase in K^{+} concentration in the supernatant) would suggest destabilization of the outer membrane, which can lead to cell death (Radniecki, et al., 2011). Background K^{+} concentrations in the solutions proved too high to observe any measureable change. Further investigations should be performed in a low K^{+} environment.

Absent Ag NP investigation

A mass balance analysis of the Ag NP solutions suggested that much of the Ag NP that was initially introduced to the solution was located in neither the supernatant nor the cell pellet (Figure 15). This effect was not observed in the data concerning Ag^{+} (Figure 16).

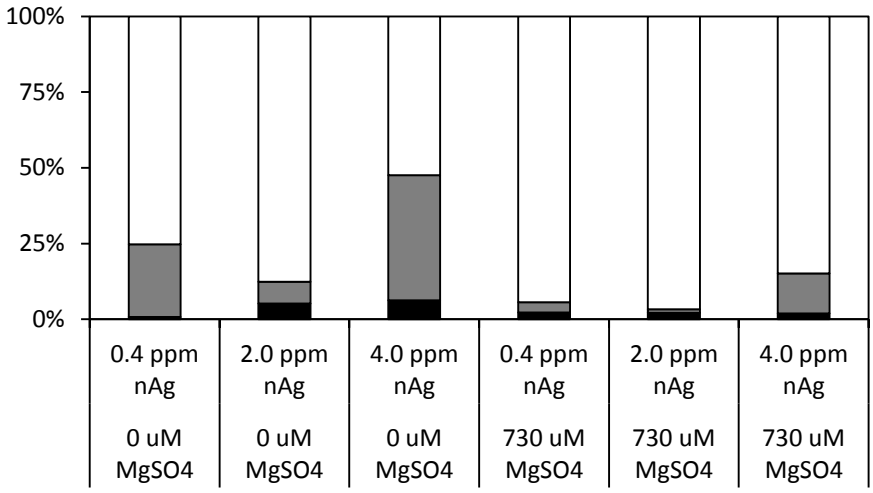

Figure 15. Location of measured Ag after 3 h inhibition experiment observing inhibitory effects of different concentrations of Ag NP in the presence and absence of 730 µM Mg^{2+}. Ag was measured in the cell pellet (■) and in the supernatant (▩). Missing Ag is also displayed (□).

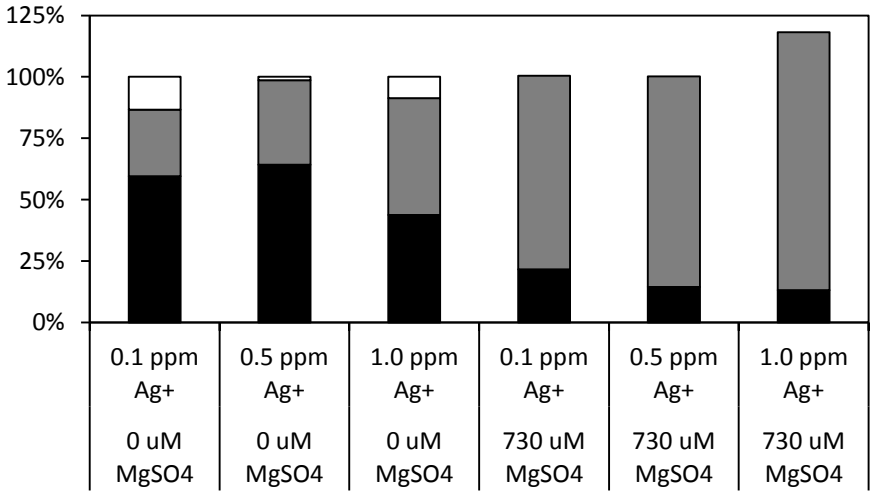

Figure 16. Location of measured Ag after 3 h inhibition experiment observing inhibitory effects of different concentrations of Ag^{+} in the presence and absence of 730 µM Mg^{2+}. Ag was measured in the cell pellet (■) and in the supernatant (▩). Missing Ag is also displayed (□).

It is hypothesized that this missing Ag was precipitated out of solution (as has been observed to happen in previous experiments) or was sorbed to the glass of the reactor. The Ag NP investigated in these experiments may be more likely to adsorb to surfaces due to the negative charge and innate hydropobic property of the organic capping agent (citrate). Since Ag^{+} is a positive ion, it would be more likely to interact with the phospholipid bilayer of the cell (which has a net negative charge) (Mclaughlin, et al., 1971). Further research should investigate the final destination of this missing Ag and identify what effect that had on the eventual toxicity to the exposed *N. europaea*. Experiments should be performed with Ag NP that have capping agents that are less hydrophobic or have a net positive charge.

Proposed Mg^{2+} protection mechanism

A mechanism of Mg^{2+}-induced prevention of Ag sorption (Figures 4, 7, & 10) could be investigated a number of different ways. A hypothesis proposed was that in normal conditions (ion, nutrient-rich environment), divalent cations, like Mg^{2+}, serve to stabilize the net negative charge of the cell's phospholipid bilayer (Mclaughlin, et al., 1971). In the absence of Mg^{2+}, or comparable nutrients, the net negative charge is readily neutralized by Ag^{+} ions, which then is in close proximity to the cell and are easily internalized. This hypothesis can be verified by measuring the cells surface charges in different Mg^{2+} and Ag^{+}-containing environments via zeta-potential. Also, Mg^{2+} associated with the cell pellet could also be quantified via ICP-OES analysis, like the Ag was in the data presented in this paper.

Ag release by aggregated Ag NP

The hypothesis that aggregated Ag NP release less Ag into solution could be tested by intentionally aggregating Ag NP (in a Mg^{2+} solution, monitored via UV-vis spectroscopy), removing the Ag NP from a sample of the liquid via centrifugal filtration, measuring the Ag concentration of the filtrate (as a baseline), introducing HEPES and $(NH_4)_2SO_4$ and monitoring

Ag release rates via centrifugal filtration and ICP-OES analysis of the filtrate. A control experiment would be run in parallel with this experiment with no Mg^{2+} present.

Experimental applications to Ag NP in WWTP

While Ag NP concentrations investigated in this study may be higher than would be typically found in many WWTP environments, the increase in the use of Ag NP shows no signs of slowing (Benn & Westerhoff, 2008) (Kulinowski, 2008), and Ag can bioaccumulate over time due to the hydraulic residence time being greater than the biomass residence time. This would lead to more exaggerated inhibitory effects than observed in this study.

CONCLUSIONS

As seen with previous research, 20 nm citrate-stabilized Ag NP proved less inhibitory than Ag^{+} on a ppm basis (Figure 6). Mg^{2+} protected *N. europaea* from Ag-induced inhibition for both Ag^{+} and Ag NP (Figure 6). These results are consistent with what has been observed in the case of both Zn^{2+} and Cd^{2+} (Radniecki, et al., 2008). The data presented in this paper illustrates the mechanisms of protection of *N. europaea* from Ag^{+} and Ag NP-induced inhibition. In the case of both Ag NP and Ag^{+}, Mg^{2+} prevented the incorporation of Ag to the *N. europaea* cells. In the case of Ag NP, Mg^{2+} induced aggregation of the particles, decreasing their surface area to volume ratio, and inhibiting the release of Ag^{+}. These findings provide insight into how Ag^{+} and Ag NP will affect WWTP processes. In harder water systems (730 μM Mg^{2+} corresponding with 72.7 ppm $CaCO_3$, or moderately hard water) less of a toxic effect will be observed on the nitrification process than in softer systems.

BIBLIOGRAPHY

Arnaout, C. L. & Gunsch, C. K., 2012. Impacts of silver nanoparticle coating on the nitrification potential of *Nitrosomonas europaea*. *Environmental Science & Technology,* Volume 46, pp. 5387-5395.

Arp, D. J. & Sayavedra-Soto, L. A., 2002. Molecular biology and biochemistry of ammonia oxidation by *Nitrosomonas europaea*.

ASTM, 2012. *E 2456-06, Standard Terminology Relating to Nanotechnology,* s.l.: s.n.

Auffan, M. et al., 2009. Towards a definition of inorganic nanoparticles from an environmental, health, and safety perspective. *Nature Nanotechnology,* Volume 4, pp. 634-641.

Benn, T. & Westerhoff, P., 2008. Nanoparticle silver released into water from commercially available sock fabrics. *Environmental Science & Technology,* pp. 4133-4139.

Choi, O. & Hu, Z., 2008. Size dependent and reactive oxygen species related to nanosilver toxicity to nitrifying bacteria.

Delay, M. et al., 2011. Interactions and stability of silver nanoparticles in the aqueous phase: Influence of natural organic matter (NOM) and ionic strength. *Journal of Chrmoatography,* 1218(27), pp. 4206-4212.

EPA, 1993. *Process Design Manual: Nitrogen control.*. Washington DC: US Environmental Protection Agency.

EPA, 2009. *Targeted National Sewage Sludge Survey Statistical Analysis Report,* Washington DC: US Environmental Protection Agency.

Giao, N. T. & Limpiyakorn, T., 2012. Inhibition kinetics of ammonia oxidation influenced by silver nanoparticles. *Water Air & Soil Pollution,* Volume 223, pp. 5197-5203.

Huynh, K. a. & Chen, K. L., 2011. Aggregation Kinetics of Citrate and Polyvinylpryrrolidone Coated Silver Nanoparticles in Monovalent and Divalent Electrolyte Solutions. *Environmental Science and Technology,* pp. 5564-5571.

Kulinowski, K. M., 2008. *Environmental Impacts of Nanosilver,* s.l.: ICON.

Mclaughlin, S. G. A., Szabo, G. & Eisenman, G., 1971. Divalent ions and the surface potential of charged phospholipid membranes. *The Journal of General Physiology,* Volume 58, pp. 667-687.

Mueller, N. C. & Nowack, B., 2008. Exposure modeling of engineered nanoparticles in the environment. *Environmental Science & Technology,* Volume 42, pp. 4447-4452.

Ostermeyer, A.-K., 2012. Influence of biological macromolecules on silver nanoparticle stability and toxicity to the ammonia oxidizing bacteria *Nitrosomonas europaea*. *Masters Thesis - San Diego State University.*

Radniecki, T. S., Semprini, L. & Dolan, M. E., 2008. Expression of merA, amoA, and hao in continuously cultured *Nitrosomonas europaea* cells exposed to zinc chloride additions. *Biotechnology and Bioengineering.*

Radniecki, T. S. et al., 2011. Influence of liberated silver from silver nanoparticles on nitrification inhibition of *Nitrosomonas europaea*. *Chemosphere.*

Roco, M. C., 2005. Environmentally Responsible Development of Nanotechnology. *Environmental Science & Technology,* Volume 39, pp. 107-112.

Seney, C. S., Gutzman, B. M. G. & H., R., 2009. Correlation of size and surface-enhanced Raman scattering activity of optical and spectroscopic properties for silver nanoparticles. *Journal of Physical Chemistry C,* 113(1), pp. 74-80.

The Project on Emerging Nanotechnologies, 2009. Nanotechnology and the Consumer.

Wiesner, M. et al., 2009. Decreasing uncertainties in assessing environmental exposure, risk, and ecological implications of nanomaterials. *Environmental Science and Technology,* 43(17), pp. 6458-6462.

Yuan, Z. et al., 2013. Interaction of silver nanoparticles with pure nitrifying bacteria. *Chemosphere,* Volume 90, pp. 1404-1411.

Zook, J. M. et al., 2011. Stable nanoparticle aggregates/agglomerates of different sizes and the effect of their size on hemolytic cytotoxicity. *Nanotoxicology,* Volume 5, pp. 517-530.

APPENDIX

Standard curves:

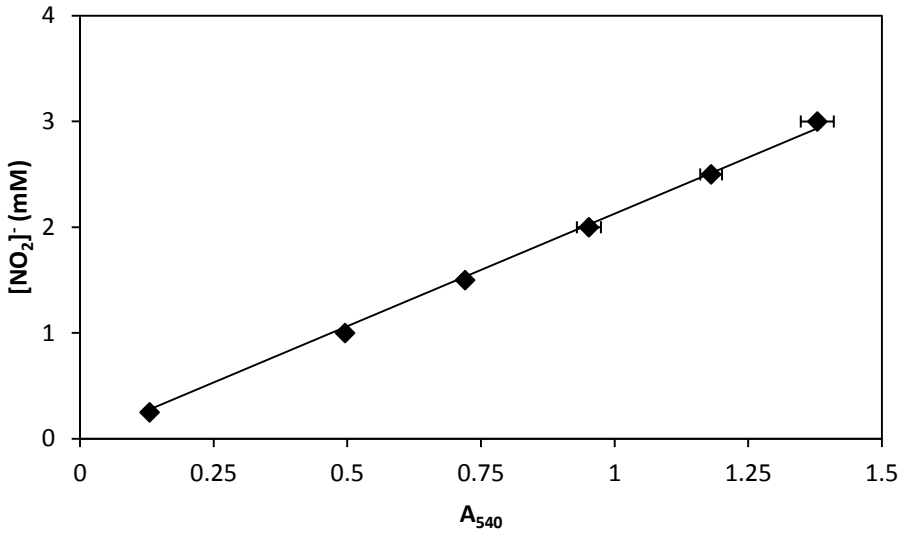

Figure 17. NO_2^- standard curve as a function of A_{540}.